

# Excellence in Chemistry Research

## Announcing our new flagship journal

- Gold Open Access
- Publishing charges waived
- Preprints welcome
- Edited by active scientists



## Meet the Editors of *ChemistryEurope*



**Luisa De Cola**

Università degli Studi  
di Milano Statale, Italy



**Ive Hermans**

University of  
Wisconsin-Madison, USA



**Ken Tanaka**

Tokyo Institute of  
Technology, Japan

## Accepted Article

**Title:** Highly efficient electrochemical ammonia synthesis via nitrate reduction over metallic Cu phase coupling sulfion degradation

**Authors:** Zhi Wang, Na Zhou, Jiazhi Wang, Depeng Wang, Jianrong Zeng, Haixia Zhong, and Xin-bo Zhang

This manuscript has been accepted after peer review and appears as an Accepted Article online prior to editing, proofing, and formal publication of the final Version of Record (VoR). The VoR will be published online in Early View as soon as possible and may be different to this Accepted Article as a result of editing. Readers should obtain the VoR from the journal website shown below when it is published to ensure accuracy of information. The authors are responsible for the content of this Accepted Article.

**To be cited as:** *ChemSusChem* **2023**, e202301050

**Link to VoR:** <https://doi.org/10.1002/cssc.202301050>

## RESEARCH ARTICLE

## Highly efficient electrochemical ammonia synthesis via nitrate reduction over metallic Cu phase coupling sulfion oxidation

Zhi Wang,<sup>+, [a, b]</sup> Na Zhou,<sup>+, [a, b]</sup> Jiazhi Wang,<sup>+, [a, b]</sup> Depeng Wang,<sup>[a, b]</sup> Jianrong Zeng,<sup>[c, d]</sup> Haixia Zhong,<sup>\*, [a, b]</sup> and Xinbo Zhang<sup>\*, [a, b]</sup>

[a] Z. Wang, N. Zhou, Dr. J. Wang, D. Wang, Prof. H. Zhong, Prof. X. Zhang  
 State Key Laboratory of Rare Earth Resource Utilization, Changchun Institute of Applied Chemistry  
 Chinese Academy of Sciences  
 5625 Renmin Street, Changchun 130022, China  
 E-mail: hxzhong@ciac.ac.cn  
 xbzhang@ciac.ac.cn

[b] Z. Wang, N. Zhou, Dr. J. Wang, D. Wang, Prof. H. Zhong, Prof. X. Zhang  
 School of Applied Chemistry and Engineering  
 University of Science and Technology of China  
 96 Jinzhai Street, Hefei 230026, China

[c] Prof. J. Zeng  
 Shanghai Synchrotron Radiation Facility, Shanghai Advanced Research Institute  
 Chinese Academy of Sciences  
 239 Zhangheng Street, Shanghai 201204, China

[d] Prof. J. Zeng  
 Shanghai Institute of Applied Physics  
 Chinese Academy of Sciences  
 2019 Jialuogong Street, Shanghai 201800, China

[+] These authors contributed equally.

Supporting information for this article is given via a link at the end of the document.

**Abstract:** Electrochemical nitrate reduction reaction (NO<sub>3</sub>RR) is a promising technology for ammonia production and denitrification of wastewater. Its application is seriously restricted by the development of the highly active and selective electrocatalyst and a rational electrolysis system. Here, we constructed an efficient electrochemical ammonia production process via nitrate reduction on the metallic Cu electrocatalyst when coupled with anodic sulfion oxidation reaction (SOR). The synthesized Cu catalyst delivers an excellent NH<sub>3</sub> Faradaic efficiency of 96.0% and a NH<sub>3</sub> yield of 0.391 mmol h<sup>-1</sup> cm<sup>-2</sup> at -0.2 V vs. reversible hydrogen electrode, which mainly stem from the more favorable conversion of NO<sub>2</sub><sup>-</sup> to NH<sub>3</sub> on Cu<sup>0</sup>. Importantly, the well-designed electrolysis system with cathodic NO<sub>3</sub>RR and anodic SOR achieves a dramatically reduced cell voltage of 0.8 V at 50 mA cm<sup>-2</sup> in comparison with the one with anodic oxygen evolution reaction (OER) of 1.9 V. This work presents an effective strategy for the energy-saving ammonia production via constructing effective nitrate reduction catalyst and replacing the OER with SOR while removing the pollutants including nitrate and sulfion.

## Introduction

Ammonia (NH<sub>3</sub>), as an indispensable feedstock for fertilizers and pharmaceuticals production, is one of the most productive chemicals.<sup>[1]</sup> Meanwhile, due to its high hydrogen content (17.8 wt.%) and relatively easy liquefaction conditions (~10 bar at room

temperature or -33 °C at atmospheric pressure), NH<sub>3</sub> is a potential hydrogen carrier and carbon-free fuel.<sup>[2]</sup> Currently, the mature industrial NH<sub>3</sub> synthesis depends on the energy-intensive Haber-Bosch (H-B) process alongside massive CO<sub>2</sub> emission.<sup>[3]</sup> Electrochemical N<sub>2</sub>/NO<sub>3</sub><sup>-</sup> reduction reaction (NRR/NO<sub>3</sub>RR) to ammonia under mild conditions using renewable electricity is increasingly being investigated as an attractive alternative.<sup>[4]</sup> Nevertheless, on account of the chemical inertness of N<sub>2</sub>, poor NH<sub>3</sub> yield and Faradaic efficiency (FE) have been achieved via NRR.<sup>[5]</sup> In contrast, owing to low dissociation energy of N=O bond, electrochemical NO<sub>3</sub>RR is more kinetically favorable.<sup>[6]</sup> Nitrate can be obtained from agricultural runoff, industrial wastewater and N<sub>2</sub> via plasma treatments.<sup>[7]</sup> Therefore, NO<sub>3</sub>RR offers a promising alternative for large-scale ammonia production and the denitrification of wastewater, wherein efficient electrocatalysts and a suitable electrolysis system are crucial.

Cu-based catalysts have been widely used for NO<sub>3</sub>RR to ammonia as a result of its moderate adsorption energy of intermediates and effective suppression of hydrogen evolution.<sup>[8]</sup> However, the sluggish kinetics of NO<sub>2</sub><sup>-</sup> intermediates conversion to NH<sub>3</sub> on Cu at low overpotential will inevitably result in the unsatisfactory ammonia production with superabundant NO<sub>2</sub><sup>-</sup> byproducts and high energy input.<sup>[8]</sup> Additionally, the effective active sites of Cu-based catalysts are still not clear owing to the unstable oxidation state and structure.<sup>[9]</sup> To solve these problems, morphology, defect, crystal plane and interface designs have

## RESEARCH ARTICLE

been developed.<sup>[10]</sup> For example, Jiang et al. constructed the Cu-Al<sub>2</sub>O<sub>3</sub> interface to stabilize the Cu<sup>δ+</sup>, which was accounted for the robust NO<sub>3</sub>RR performance.<sup>[11]</sup> Conversely, Zhou et al. proposed that Cu<sup>0</sup> is the real active phase for the highly selective NO<sub>3</sub>RR to NH<sub>3</sub>.<sup>[9]</sup> Based on our density functional theory (DFT) calculations, we found that the NO<sub>3</sub><sup>-</sup> adsorption on Cu<sub>2</sub>O is stronger than on Cu and the NH<sub>3</sub> desorption on Cu is far more efficient on Cu<sub>2</sub>O (Figures 1 and S1). It means that the stable Cu<sup>0</sup> at the reduction potential can achieve a more favorable conversion of NO<sub>3</sub><sup>-</sup> to NH<sub>3</sub> than the unstable Cu<sup>+</sup>. Thus, developing metallic Cu catalysts is desirable for NO<sub>3</sub>RR to ammonia yet very challenging.

In addition to the ungratified NO<sub>3</sub>RR catalyst design, the energy-efficient ammonia production is also restricted by anodic oxygen evolution reaction (OER) due to its high potential (0.401 V vs. SHE, pH=14) and the slow multiple proton-coupled electron-transfer kinetics.<sup>[12]</sup> It is necessary to substitute OER with more favorable anodic oxidation reaction for highly efficient ammonia production with reduced cell voltage, such as sulfion oxidation reaction (SOR) with lower oxidation potential (S<sup>2-</sup> - 2e<sup>-</sup> = S, -0.48 V vs. SHE, pH=14).<sup>[13]</sup> Moreover, this electrochemical SOR also affords a sustainable avenue to convert the toxic pollutants (e. g. H<sub>2</sub>S or S<sup>2-</sup>) from oil refineries and nature-gas extraction industries to harmless elemental sulfur.<sup>[14]</sup> Therefore, the system coupling NO<sub>3</sub>RR with SOR is attractive for the lower-cost and high-efficiency NH<sub>3</sub> production and pollutant degradation.

Herein, we demonstrated that the selective and low-energy NH<sub>3</sub> synthesis can be built through the promoted NO<sub>3</sub><sup>-</sup> reduction on the cathodic metallic Cu catalyst and replacing the traditional OER with SOR. Density functional theory (DFT) calculations show that the NO<sub>2</sub><sup>-</sup> conversion to NH<sub>3</sub> on metallic Cu phase is more favorable than that on Cu<sub>2</sub>O. The synthesized metallic Cu electrocatalyst presents a NH<sub>3</sub> Faradaic efficiency of 96.0% and a NH<sub>3</sub> yield of 0.391 mmol h<sup>-1</sup> cm<sup>-2</sup> at a low potential of -0.2 V vs. RHE, which is better than these Cu<sub>2</sub>O catalysts. Coupling NO<sub>3</sub>RR with SOR, NH<sub>3</sub> production was proceed at an ultralow cell voltage of 1.2 V at the current density of around 85 mA cm<sup>-2</sup> in two-electrode electrolysis system. A notable reduction of 50% in the cell voltage is observed for the NO<sub>3</sub>RR-SOR system (1.2 V) with respect to the NO<sub>3</sub>RR-OER one (2.387 V). Our findings provide a general strategy for developing metal Cu catalyst and energy-saving ammonia synthesis process as well.

## Results and Discussion

On basis of DFT results, metal Cu particles were synthesized for electrocatalytic nitrate reduction to ammonia. To alleviate the formation of oxide phases, a chemical reduction and precipitation process was rapidly finished to synthesize the Cu catalysts (CR-Cu). As shown by the transmission electron microscopy (TEM) image, the selected area electron diffraction (SAED) pattern and the scanning electron microscopy (SEM) image, CR-Cu is polycrystalline with an average particle size of ~28.8 nm (Figures 2a and S2). Clear lattice spacing of 2.08 Å is found in the high-resolution transmission electron microscopy (HRTEM) image of CR-Cu, which corresponds to Cu(111) (Figure 2b). Through the scanning transmission electron microscopy-energy dispersive X-

ray spectroscopy (STEM-EDX) elemental mapping analysis, trace surface oxygen element despite Cu element was detected for CR-Cu (Figure 2c-e), which is likely associated with the surface oxidation of Cu nanoparticles.

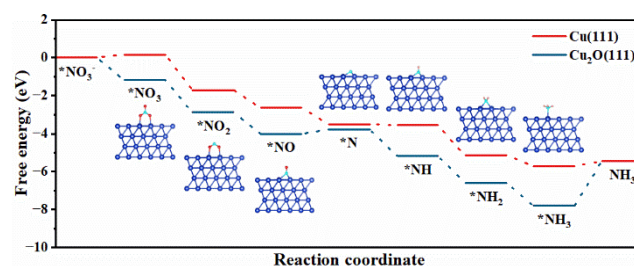


**Figure 1.** The calculated Gibbs free energy diagrams for NO<sub>3</sub><sup>-</sup>-to-NH<sub>3</sub> conversion on Cu and Cu<sub>2</sub>O catalyst. The blue, red, cyan and pink balls represent copper, oxygen, nitrogen and hydrogen atoms, respectively.

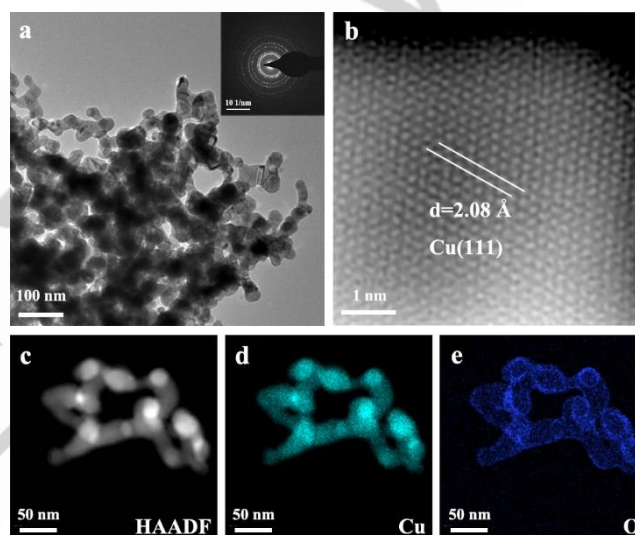


**Figure 2.** (a) TEM image and the corresponding SAED pattern (insert) of CR-Cu. (b) HRTEM image of CR-Cu. (c) HAADF-STEM image and EDX elemental mapping of Cu (d) and O (e) elements in CR-Cu.

However, the X-ray diffraction (XRD) patterns illustrate no obvious characteristic peaks of oxide phases for CR-Cu compared with the commercial Cu particles with minimal Cu<sub>2</sub>O peaks at 36.6°, 42.5° and 61.6° (Figure 3a). Nevertheless, the X-ray photoelectron spectroscopy (XPS) spectrum indicates the existence of Cu and O element for CR-Cu (Figure S3), which is consisted with the EDX analysis. Figure 3b shows the high-resolution Cu 2p spectrum of CR-Cu. Two set of peaks at 932.6 and 952.3 eV are assigned to Cu 2p<sub>3/2</sub> and Cu 2p<sub>1/2</sub>, respectively. The according deconvoluted spectrum indicates the existence of Cu<sup>0</sup>/Cu<sup>+</sup> of CR-Cu.<sup>[15]</sup> The high-resolution Cu LMM Auger electron spectroscopy (AES) spectra of CR-Cu further reflect that the content of external Cu<sup>+</sup> to Cu<sup>0</sup> and certify the presence of amorphous oxide phases, which cannot be detected by XRD

## RESEARCH ARTICLE

(Figure 3c).<sup>[16]</sup> In addition, X-ray absorption spectroscopy (XAS) analyses were performed to further investigate the chemical state of the Cu atoms in the CR-Cu sample. As shown in Figure S4, The Cu K-edge X-ray absorption near-edge structure (XANES) spectra indicate that CR-Cu exhibits a similar typical  $\text{Cu}^0$  peak compared to the reference Cu foil, which is different from the  $\text{Cu}_2\text{O}$ .<sup>[17]</sup> Notably, the minimal positive shift of these peak of CR-Cu compared to Cu foil reference was due to the partial oxidation of CR-Cu, which is consisted with the XPS results. The Fourier-transformed extended X-ray absorption fine structure (FT-EXAFS) in Figure 3d further elucidates the Cu-O and Cu-Cu configuration of CR-Cu.<sup>[16a]</sup> It is thus clear that CR-Cu with slightly oxidation was successfully synthesized.<sup>[18]</sup>

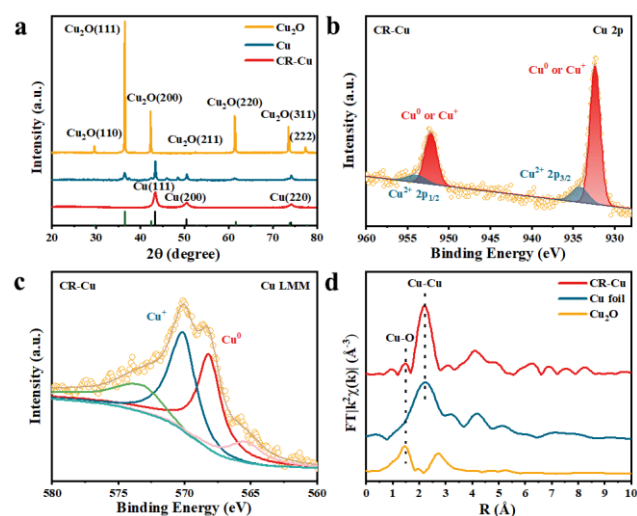


**Figure 3.** (a) XRD patterns of  $\text{Cu}_2\text{O}$ , Cu and CR-Cu. (b) Cu 2p XPS spectra and (c) Cu LMM AES spectra of CR-Cu. (d) FT-EXAFS spectra of CR-Cu, Cu foil, and  $\text{Cu}_2\text{O}$ .

Regarding the presence of surface Cu-based oxides, CR-Cu was further treated by an electrochemical reduction method (abbreviated as ER-Cu, Figures S5 and S6).<sup>[9]</sup> To evaluate the  $\text{NO}_3\text{RR}$  performance of these Cu catalysts, chronoamperometry tests were conducted in 1 M KOH electrolyte with 0.1 M  $\text{KNO}_3$ . The products were detected by UV-vis photometer and ion chromatography (Figures S7 and S8). As shown in Figure 4a, ER-Cu exhibits higher  $\text{NH}_3$  selectivity with larger Faradaic efficiency than CR-Cu and  $\text{Cu}_2\text{O}$  over the overall applied potentials. At  $-0.2$  V vs. RHE, ER-Cu reaches a maximum  $\text{NH}_3$  Faradaic efficiency up to 96.0%, superior to CR-Cu (81.5%) and  $\text{Cu}_2\text{O}$  (76.3%), as well as other similar Cu-based electrocatalyst (Figure S9 and Table S1). Accordingly, the calculated molar concentration ratios of  $\text{NH}_3$  to  $\text{NO}_2^-$  for these samples are shown in Figure 4b. Upon increasing the applied reduction potentials, the ratio of  $\text{NH}_3$  for all these samples increases due to the accelerated reduction of  $\text{NO}_2^-$  to  $\text{NH}_3$  at high overpotential. Larger molar ratio of  $\text{NH}_3$  to  $\text{NO}_2^-$  is observed on ER-Cu compared to CR-Cu and  $\text{Cu}_2\text{O}$ . Thus, the conversion of  $\text{NO}_2^-$  to  $\text{NH}_3$  on metallic Cu phase is more favorable, which is consisted with the DFT calculations. The  $\text{NH}_3$  yield for all the samples increases upon varying the applied potential from 0

to  $-0.3$  V vs. RHE as well. The  $\text{NH}_3$  yield for ER-Cu was calculated to be  $0.391 \text{ mmol h}^{-1} \text{ cm}^{-2}$  at  $-0.2$  V vs. RHE, which outcompetes CR-Cu ( $0.278 \text{ mmol h}^{-1} \text{ cm}^{-2}$ ) and  $\text{Cu}_2\text{O}$  ( $0.146 \text{ mmol h}^{-1} \text{ cm}^{-2}$ ) (Figure 4c). To prove that  $\text{NH}_3$  originates from specific reactants, isotope labelling experiments were conducted using  $^{15}\text{NO}_3^-$  and  $^{14}\text{NO}_3^-$  as the nitrogen source, respectively. Two typical peaks of  $^{15}\text{NH}_4^+$  or three typical peaks of  $^{14}\text{NH}_4^+$  are individually observed in the  $^1\text{H}$  NMR spectra of the electrolyte using  $^{15}\text{NO}_3^-$  and  $^{14}\text{NO}_3^-$ , confirming that  $\text{NO}_3^-$  in the electrolyte is the nitrogen source (Figure 4d) for ammonia generation.<sup>[19]</sup>

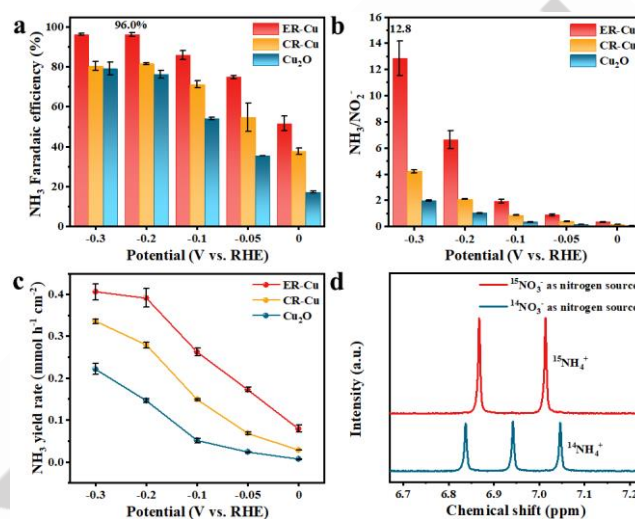


**Figure 4.** (a) Faradaic efficiency of  $\text{NH}_3$  at various potentials for ER-Cu, CR-Cu and  $\text{Cu}_2\text{O}$ . (b) Molar concentration ratio of  $\text{NH}_3$  to  $\text{NO}_2^-$  at different potentials for ER-Cu, CR-Cu and  $\text{Cu}_2\text{O}$ . (c) Yield rate of  $\text{NH}_3$  at various potentials for ER-Cu, CR-Cu and  $\text{Cu}_2\text{O}$ . (d)  $^1\text{H}$  NMR spectra of  $^{15}\text{NH}_4^+$  and  $^{14}\text{NH}_4^+$  produced after  $\text{NO}_3\text{RR}$  over ER-Cu electrode using  $^{15}\text{NO}_3^-$  and  $^{14}\text{NO}_3^-$  as the nitrogen source, respectively.

For the practical  $\text{NH}_3$  production, low energy input is necessary. Given that high potential is required to drive OER, anodic SOR is considered to reduce the overall electrolysis cell voltage. CR-Cu after the electrochemically sulfurization (ES-Cu) was not used for SOR due to its unsatisfactory catalytic performance (Figure S14). Here, the typically active anodic oxidation electrocatalyst, such as Ni/Fe hydroxides on Ni foam, was chosen to replace the Pt counter electrode considering the high catalytic performance of Ni/Fe sites toward the anodic oxidation reactions.<sup>[20]</sup> The anode with excellent SOR activity was prepared by doping S into the typically OER active Ni/Fe hydroxide [ $\text{S}-(\text{Ni},\text{Fe})\text{O}_x\text{H}_y$ ] on Ni foam, as manifested by XRD, SEM, SAED, TEM-EDX, XPS spectra and linear sweep voltammetry (see detailed discussion in Supporting Information, Figures S10-14).<sup>[21]</sup> The polarization curves (Figure 5a) uncover that the onset potentials of SOR and OER are 0.288 and 1.366 V vs. RHE, respectively. Such a low onset potential of SOR is undoubtedly conducive to reducing the energy demand of  $\text{NH}_3$  production. The long-term stability of SOR on  $\text{S}-(\text{Ni},\text{Fe})\text{O}_x\text{H}_y$  electrode was tested at  $100 \text{ mA cm}^{-2}$  for 24 h (Figure S15). The activity of the catalyst remains stable, evidencing the good stability of the S-doped Ni/Fe hydroxide. The UV-vis spectra of

## RESEARCH ARTICLE

the electrolyte during the 8 h SOR test at  $100 \text{ mA cm}^{-2}$  showcase the absorption peaks at 300 and 370 nm, certifying the formation of polysulfides products ( $\text{S}_x^{2-}$ ,  $2 \leq x \leq 4$ ) (Figure S16a).<sup>[22]</sup> After 8-hours SOR test, the electrolyte turned brown and the polysulfides in electrolyte were treated with acid to obtain the pale-yellow S powder, which was indicated by XRD analysis (Figure S16b).<sup>[23]</sup> Thus, substituting the OER with SOR is feasible for reducing the energy input for the electrochemical  $\text{NH}_3$  synthesis.

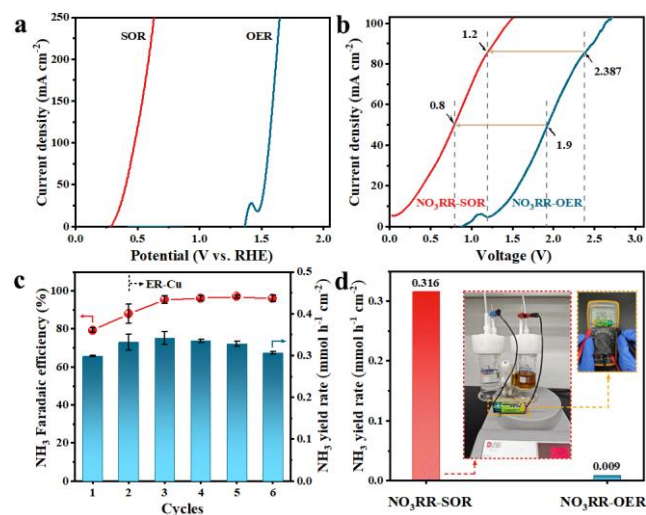


**Figure 5.** (a) Polarization curves of SOR on the S-(Ni,Fe)O<sub>x</sub>H<sub>y</sub> electrode and polarization curves of OER on the (Ni,Fe)O<sub>x</sub>H<sub>y</sub> electrode. (b) Polarization curves of the two-electrode NO<sub>3</sub>RR-SOR and NO<sub>3</sub>RR-OER systems. (c) Cyclability test of the two-electrode NO<sub>3</sub>RR-SOR system at 1.2 V with CR-Cu as cathode and S-(Ni,Fe)O<sub>x</sub>H<sub>y</sub> as anode. (d) NH<sub>3</sub> yield rate of two-electrode systems driven by a commercial battery with the nominal voltage of 1.2 V and the photo of corresponding NO<sub>3</sub>RR-SOR system.

Two-electrode systems of the cathodic NO<sub>3</sub>RR with anodic SOR or OER were further used for NH<sub>3</sub> synthesis. The polarization curves suggest that the cell voltages of 1.2 and 2.387 V are severally required to reach the same current density of around  $85 \text{ mA cm}^{-2}$  for the NO<sub>3</sub>RR-SOR and NO<sub>3</sub>RR-OER system (Figure 5b). The reduction of 50% about cell voltage corresponds to the significant energy saving. The cycling stability test of two-electrode NO<sub>3</sub>RR-SOR system with cathodic metallic Cu catalyst was carried out (Figure 5c) at the cell voltage of 1.2 V. After the second cycle, the Faradaic efficiency of NH<sub>3</sub> maintains around 95%, which is associated with the conversion of CR-Cu to ER-Cu and more favorable ammonia generation process. Meanwhile, the characterizations of ER-Cu after the long-term durability test are shown in Figure S17 and S18. Results illustrate the maintained structure and morphology of ER-Cu, accompany with slight particle fragmentation and reaggregation after the long-term durability test, corroborating the good stability of the metallic Cu catalyst. More importantly, the efficient ammonia production can be driven by a commercial battery with the nominal voltage of 1.2 V (Figures 5d and S19). And the NH<sub>3</sub> yield rate is  $0.316 \text{ mmol h}^{-1} \text{ cm}^{-2}$  for this NO<sub>3</sub>RR-SOR system. Meanwhile, only negligible

amount of NH<sub>3</sub> was generated in the NO<sub>3</sub>RR-OER system driven by this commercial battery.

## Conclusion

In conclusion, we attested to the efficient nitrate reduction to NH<sub>3</sub> on metallic Cu electrocatalyst and realized an energy-saving ammonia production system of cathodic NO<sub>3</sub>RR and anodic SOR. Due to the more favorable conversion NO<sub>2</sub><sup>-</sup> to NH<sub>3</sub>, the metallic Cu catalyst synthesized by a chemical and electrochemical reduction approach achieves a high NH<sub>3</sub> Faradaic efficiency of 96.0% and a NH<sub>3</sub> yield of  $0.391 \text{ mmol h}^{-1} \text{ cm}^{-2}$  at a low potential of -0.2 V vs. RHE. By virtue of the lower onset potential of SOR compared to OER, the efficient NH<sub>3</sub> production via NO<sub>3</sub>RR integrated with anodic SOR was obtained, presenting a NH<sub>3</sub> Faradaic efficiency of around 95% at a smaller cell voltage of 1.2 V. This signifies a 50% decrease in cell voltage relative to the NO<sub>3</sub>RR-OER system. Our findings will offer guidance on the rational design of nitrate reduction catalysts and the effective strategy for energy-saving electrolysis process via utilizing the more thermodynamically and kinetically favorable anodic reaction, as well as a sustainable route for the removal of water pollutants.

## Supporting Information

The authors have cited additional references within the Supporting Information.<sup>[24-29]</sup>

## Acknowledgements

This work was supported by National Key R&D Program of China (2021YFB4000402), the National Natural Science Foundation of China (52071311, 52273277, 52072362), Jilin Province Science and Technology Development Plan Funding Project (20220201112GX) and Youth Innovation Promotion Association CAS (2020230 and 2021223). H.X.Z. acknowledges funding from National Natural Science Foundation of China Outstanding Youth Science Foundation of China (Overseas). These authors thank the staff of beamline BL13SSW at Shanghai Synchrotron Radiation Facility for experiments supports.

**Keywords:** nitrate reduction • ammonia production • metallic Cu electrocatalyst • sulfion oxidation • energy-saving

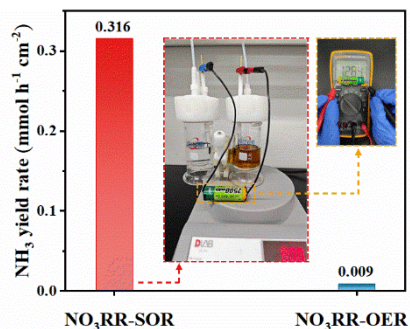
- [1] a) V. Rosca, M. Duca, M. T. de Groot, M. T. M. Koper, *Chem. Rev.* **2009**, *109*, 2209-2244; b) T. Ren, Z. Yu, H. Yu, K. Deng, Z. Wang, X. Li, H. Wang, L. Wang, Y. Xu, *Appl. Catal. B Environ.* **2022**, *318*, 121805.
- [2] a) Y. Gao, Q. Xia, L. Hao, A. W. Robertson, Z. Sun, *ACS Sustain. Chem. Eng.* **2022**, *10*, 1316-1322; b) D. R. MacFarlane, P. V. Cherepanov, J. Choi, B. H. R. Suryanto, R. Y. Hodgetts, J. M. Bakker, F. M. F. Vallana, A. N. Simonov, *Joule* **2020**, *4*, 1186-1205.
- [3] N. C. Kani, N. H. L. Nguyen, K. Markel, R. R. Bhawnani, B. Shindel, K. Sharma, S. Kim, V. P. Dravid, V. Berry, J. A. Gauthier, M. R. Singh, *Adv. Energy Mater.* **2023**, *13*, 2204236.

## RESEARCH ARTICLE

- [4] J. Li, G. M. Zhan, J. H. Yang, F. J. Quan, C. L. Mao, Y. Liu, B. Wang, F. C. Lei, L. J. Li, A. W. M. Chan, L. P. Xu, Y. B. Shi, Y. Du, W. C. Hao, P. K. Wong, J. F. Wang, S. X. Dou, L. Z. Zhang, J. C. Yu, *J. Am. Chem. Soc.* **2020**, *142*, 7036-7046.
- [5] a) Y. Wang, H. Li, W. Zhou, X. Zhang, B. Zhang, Y. Yu, *Angew. Chem. Int. Ed.* **2022**, *61*, e202202604; b) Z. Deng, J. Liang, Q. Liu, C. Ma, L. Xie, L. Yue, Y. Ren, T. Li, Y. Luo, N. Li, B. Tang, A. Ali Alshehri, I. Shakir, P. O. Agboola, S. Yan, B. Zheng, J. Du, Q. Kong, X. Sun, *Chem. Eng. J.* **2022**, *435*, 135104.
- [6] F. Lv, M. Z. Sun, Y. P. Hu, J. Xu, W. Huang, N. Han, B. L. Huang, Y. G. Li, *Energy Environ. Sci.* **2023**, *16*, 201-209.
- [7] a) Q. Gao, H. S. Pillai, Y. Huang, S. K. Liu, Q. M. Mu, X. Han, Z. H. Yan, H. Zhou, Q. He, H. L. Xin, H. Y. Zhu, *Nat. Commun.* **2022**, *13*, 2338; b) X. Zhang, Y. T. Wang, C. B. Liu, Y. F. Yu, S. Y. Lu, B. Zhang, *Chem. Eng. J.* **2021**, *403*, 126269.
- [8] a) H. M. Liu, X. Y. Lang, C. Zhu, J. Timoshenko, M. Rüscher, L. C. Bai, N. Guijarro, H. B. Yin, Y. Peng, J. H. Li, Z. Liu, W. C. Wang, B. Roldan Cuenya, J. S. Luo, *Angew. Chem. Int. Ed.* **2022**, *61*, e202202556; b) W. D. Wen, P. Yan, W. P. Sun, Y. T. Zhou, X. Y. Yu, *Adv. Funct. Mater.* **2023**, *33*, 2212236.
- [9] N. Zhou, Z. Wang, N. Zhang, D. Bao, H. X. Zhong, X. B. Zhang, *ACS Catal.* **2023**, *13*, 7529-7537.
- [10] a) X. B. Fu, X. G. Zhao, X. B. Hu, K. He, Y. N. Yu, T. Li, Q. Tu, X. Qian, Q. Yue, M. R. Wasielewski, Y. J. Kang, *Appl. Mater. Today* **2020**, *19*, 100620; b) R. R. Jia, Y. T. Wang, C. H. Wang, Y. F. Ling, Y. F. Yu, B. Zhang, *ACS Catal.* **2020**, *10*, 3533-3540; c) S. B. Patil, T.-R. Liu, H.-L. Chou, Y.-B. Huang, C.-C. Chang, Y.-C. Chen, Y.-S. Lin, H. Li, Y.-C. Lee, Y. J. Chang, Y.-H. Lai, C.-Y. Wen, D.-Y. Wang, *J. Phys. Chem. Lett.* **2021**, *12*, 8121-8128.
- [11] G. Jiang, M. Peng, L. Hu, J. Ouyang, X. Lv, Z. Yang, X. Liang, Y. Liu, H. Liu, *Chem. Eng. J.* **2022**, *435*, 134853.
- [12] a) L. Y. Zhang, Z. Y. Wang, J. S. Qiu, *Adv. Mater.* **2022**, *34*, e2109321; b) Y. H. Pei, J. Cheng, H. Zhong, Z. F. Pi, Y. Zhao, F. M. Jin, *Green Chem.* **2021**, *23*, 6975-6983.
- [13] L. Yi, Y. Ji, P. Shao, J. Chen, J. Li, H. Li, K. Chen, X. Peng, Z. Wen, *Angew. Chem. Int. Ed.* **2021**, *60*, 21550-21557.
- [14] K. X. Yang, N. Zhang, J. F. Yang, Z. Xu, J. Q. Yan, D. Li, S. Z. Liu, *Appl. Catal. B Environ.* **2023**, *332*, 122718.
- [15] T. Zhao, J. Li, J. Liu, F. Liu, K. Xu, M. Yu, W. Xu, F. Cheng, *ACS Catal.* **2023**, *13*, 4444-4453.
- [16] a) X. T. Li, Q. Liu, J. H. Wang, D. C. Meng, Y. J. Shu, X. Z. Lv, B. Zhao, H. Yang, T. Cheng, Q. S. Gao, L. S. Li, H. B. Wu, *Chem* **2022**, *8*, 2148-2162; b) Z. Y. Zhao, X. T. Li, J. H. Wang, X. Z. Lv, H. B. Wu, *Journal of CO<sub>2</sub> Utilization* **2021**, *54*, 101741.
- [17] Y. Zhou, F. Che, M. Liu, C. Zou, Z. Liang, P. De Luna, H. Yuan, J. Li, Z. Wang, H. Xie, H. Li, P. Chen, E. Bladt, R. Quintero-Bermudez, T.-K. Sham, S. Bals, J. Hofkens, D. Sinton, G. Chen, E. H. Sargent, *Nat. Chem.* **2018**, *10*, 974-980.
- [18] K. Yao, J. Li, H. Wang, R. Lu, X. Yang, M. Luo, N. Wang, Z. Wang, C. Liu, T. Jing, S. Chen, E. Cortés, S. A. Maier, S. Zhang, T. Li, Y. Yu, Y. Liu, X. Kang, H. Liang, *J. Am. Chem. Soc.* **2022**, *144*, 14005-14011.
- [19] H. Du, H. Guo, K. Wang, X. Du, B. A. Beshiwork, S. Sun, Y. Luo, Q. Liu, T. Li, X. Sun, *Angew. Chem. Int. Ed.* **2022**, *62*, e202215782.
- [20] a) M. B. Stevens, C. D. M. Trang, L. J. Enman, J. Deng, S. W. Boettcher, *J. Am. Chem. Soc.* **2017**, *139*, 11361-11364; b) M. Cai, Q. Zhu, X. Wang, Z. Shao, L. Yao, H. Zeng, X. Wu, J. Chen, K. Huang, S. Feng, *Adv. Mater.* **2022**, *35*, 2209338; c) L. Y. Zeng, Y. J. Chen, M. Z. Sun, Q. Z. Huang, K. A. Sun, J. Y. Ma, J. Li, H. Tan, M. G. Li, Y. Pan, Y. Q. Liu, M. C. Luo, B. L. Huang, S. J. Guo, *J. Am. Chem. Soc.* **2023**, *145*, 17577-17587.
- [21] L. Yu, L. B. Wu, B. McElhenny, S. W. Song, D. Luo, F. H. Zhang, Y. Yu, S. Chen, Z. F. Ren, *Energy Environ. Sci.* **2020**, *13*, 3439-3446.
- [22] a) M. Zhang, J. Guan, Y. C. Tu, S. M. Chen, Y. Wang, S. H. Wang, L. Yu, C. Ma, D. H. Deng, X. H. Bao, *Energy Environ. Sci.* **2020**, *13*, 119-126; b) Z. H. Xiao, C. Lu, J. Wang, Y. Y. Qian, B. W. Wang, Q. Zhang, A. D. Tang, H. M. Yang, *Adv. Funct. Mater.* **2023**, *33*, 2212183.
- [23] a) Q. Zhang, I. G. Dalla Lana, K. T. Chuang, H. Wang, *Ind. Eng. Chem. Res.* **2000**, *39*, 2505-2509; b) J. P. Fornés, J. M. Bisang, *Electrochim. Acta* **2017**, *243*, 90-97; c) C. Lyu, Y. Li, J. Cheng, Y. Yang, K. Wu, J. Wu, H. Wang, W. M. Lau, Z. Tian, N. Wang, J. Zheng, *Small* **2023**, *19*, 2302055.
- [24] S. Zhang, J. H. Wu, M. T. Zheng, X. Jin, Z. H. Shen, Z. H. Li, Y. J. Wang, Q. Wang, X. B. Wang, H. Wei, J. W. Zhang, P. Wang, S. Q. Zhang, L. Y. Yu, L. F. Dong, Q. S. Zhu, H. G. Zhang, J. Lu, *Nat. Commun.* **2023**, *14*, 3634.
- [25] J. Yang, H. F. Qi, A. Q. Li, X. Y. Liu, X. F. Yang, S. X. Zhang, Q. Zhao, Q. K. Jiang, Y. Su, L. L. Zhang, J. F. Li, Z. Q. Tian, W. Liu, A. Q. Wang, T. Zhang, *J. Am. Chem. Soc.* **2022**, *144*, 12062-12071.
- [26] R. Daiyan, T. Tran-Phu, P. Kumar, K. Iputera, Z. Tong, J. Leverett, M. H. A. Khan, A. Asghar Esmailpour, A. Jalili, M. Lim, A. Tricoli, R.-S. Liu, X. Lu, E. Lovell, R. Amal, *Energy Environ. Sci.* **2021**, *14*, 3588-3598.
- [27] Y. T. Wang, W. Zhou, R. R. Jia, Y. F. Yu, B. Zhang, *Angew. Chem. Int. Ed.* **2020**, *59*, 5350-5354.
- [28] J. S. Li, J. F. Gao, T. Z. Feng, H. H. Zhang, D. P. Liu, C. M. Zhang, S. Y. Huang, C. H. Wang, F. Du, C. M. Li, C. X. Guo, *J. Power Sources* **2021**, *511*, 230463.
- [29] A. Paliwal, C. D. Bendas, E. S. Thornburg, R. T. Haasch, A. A. Gewirth, *ACS Catal.* **2023**, *13*, 6754-6762.

## RESEARCH ARTICLE

## Entry for the Table of Contents



The efficient nitrate reduction to ammonia on metallic Cu phase was realized. The cell voltage was significantly reduced through an energy-saving ammonia production system of cathodic nitrate reduction reaction (NO<sub>3</sub>RR) and anodic sulfion oxidation reaction (SOR) rather than oxygen evolution reaction (OER). Note that the efficient ammonia synthesis can be driven by a 1.2 V commercial battery.